STATUS OF UV-FIBERS
FOR APPLICATIONS BELOW 250 nm

Karl-Friedrich Klein
Fachhochschule/University of Applied Sciences Giessen-Friedberg
Wilhelm-Leuschner-Straße 13, 61169 Friedberg, Germany
e-mail: Karl-Friedrich.Klein@e2.fh-friedberg.de,
Tel: (+49) 6031 604 214, Fax: (+49) 6031 604-180

ABSTRACT

Mainly due to the unexpected progress in manufacturing of solarization-reduced all-silica fibers, new fiber-optic applications in the UV-region are feasible. However, the other components like the UV-sources and the detector-systems have to be improved, too. Especially, the miniaturization is very important fitting to the small-sized fiber-optic assemblies leading to compact and mobile UV-analytical systems.

Based on independent improvements in the preform and fiber processing, UV-improved fibers with different properties have been developed. The best UV-fiber for the proposed applications is selectable by its short and long-term spectral behavior, especially in the region from 190 to 350 nm. The spectrum of the UV-source and the power density in the fiber have an influence on the nonlinear transmission and the damaging level; however, hydrogen can reduce the UV-defect concentration. After determining the diffusion processes in the fiber, the UV-lifetime in commercially available all-silica fibers can be predicted. Newest results with light from deuterium-lamps, excimer-lasers and 5th harmonics of Nd-YAG-laser will be shown.

Finally, some new applications with UV-fiber optics will be shown; especially the TLC-method can be improved significantly, combining a 2-row fiber-array with a diode-array spectrometer optimized for fiber-optics

KEYWORDS: all-silica fibers, Teflon-fibers, UV-defects, solarization, linear and non-linear transmission, fiber-optic application, thin layer chromatography

1. INTRODUCTION

For more than a decade, fiber-optic systems have been commercially available. Given by the existing components, the applications were mainly restricted to the UV-VIS- and NIR-region. Outside these regions, above 2.5 µm and below 250 nm, the performance of the optical fibers based on silica was not sufficient at that time.

In meantime, there are two attractive possibilities in the DUV-region below 250 nm: the hollow-core wave-guides /1,2/ or all-silica multimode fibers with undoped synthetic core having high OH-content and fluorine doped cladding /3,4,5/. The breakthrough for the solid core fibers in this UV-region was realized by passivation /6,7/ of UV-defects /8,9/ generated during UV-light transportation, using different UV-light sources, e.g. deuterium-lamp, excimer-lasers, frequency doubled Argon-laser, 4th harmonic of Nd-YAG-lasers (see also references in /7,10/).

In parallel, the preform material has been improved significantly /11/; however, UV-defects are still generated in this material.

In addition to the improvements of UV-fibers, new UV-sources and detector-systems have been developed forced by new applications. Especially for mobile systems, compact components in combination with optical fibers are requested. For UV-spectroscopy, either a broadband light-source like a deuterium-lamp /12/ or UV-lasers (see above) are mainly used in laboratory under controlled conditions. Therefore, miniaturization of light sources with reduced power was the main concern for mobil systems. In meantime, commercial products with significantly smaller dimensions were presented at the LASER'99 in Munich fulfilling these requirements: e.g. a mini-deuterium-lamp /12/ or Nd-YAG-lasers /13/ with 355 or 266 nm wavelength. For spectral analyses, fiber-optic spectrometers /14,15/ have been optimized during the last years, including the DUV-region.

In the following, we will describe the status of the UV-improved all-silica fibers taking into account the requirements from the applications. The first results of a high-NA fiber for the DUV-region will be presented, too.

For a mobile system, the mini-deuterium-lamp has been tested. Especially for periodic operation, the advantages of this lamp will be shown. Finally, we will point out some applications which seem to be realizable because of UV-fiber improvements.

2. MEASUREMENT-SYSTEMS AND RESULTS

2.1. Fiber samples and measurement techniques

In these studies, we used all-silica fibers manufactured at Polymicro Technologies /5/. In order to show the current status, the fibers were drawn from the improved preform having undoped silica core and fluorine-doped silica cladding described above. The coating material was Polyimide /5/. The test length of 2 m was mainly fixed. For comparison in these tests, the core diameter of the so-called UVM-fibers was different as follows: 70, 100, 200, 400 and 600 µm. A part of the fibers had been loaded with hydrogen, too; these fibers are called UVMI-fibers.
Parallel to these all-silica fibers with small cladding-to-core ratio (CCR < 1.2), PCS-fibers with a silica core and a polymer cladding made from Teflon-AF were drawn and loaded with hydrogen; however, the core material is the standard Suprasil-material having a higher content of defects.
Finally, all fibers have been connectorized on both sides with SMA-connectors, which were marked as described in /16/.

To determine the temporal behavior of the UV-defects, we used our standard UV-equipment with the following components: a standard 30W-deuterium-lamp with a broadband UV-spectrum; an optimized imaging-system for damaging-tests, two coupling-units with SMA-couplers, a fiber-optic UV-spectrometer with CCD-array. A more detailed description, especially about the input spectral power, is given in /7,14/.

2.2. Experimental results with deuterium-lamp

In high-OH silica fibers, UV-light can generate UV-defects in silica networks. Mainly the E'-center with an absorption band at 215 nm is disturbing; the mechanism of generation is shown with eq.(1) and (2):

$$\equiv \mathrm{Si} - \mathrm{O} - \mathrm{Si} \equiv \quad + h\nu \quad \rightarrow \quad \equiv \mathrm{Si}^{\bullet} \quad {}^{\circ}\mathrm{O} - \mathrm{Si} \equiv \tag{1}$$

$$\equiv \mathrm{Si} - \mathrm{Cl} \quad + h\nu \quad \rightarrow \quad \equiv \mathrm{Si}^{\bullet} \quad \mathrm{Cl}^{\circ} \tag{2}$$

Although the chlorine-content is small, in comparison to the OH-content, this breakage of bonds seems to be dominant: only a small NBOHC-band at 266 nm is seen which should be generated by eq. (1), too.
However, molecular hydrogen can reduce the amount of defects significantly by passivation of the UV-defects described above, as shown in equation (3):

$$\equiv \mathrm{Si}^{\bullet} + \mathrm{H}_2 \quad \rightarrow \quad \equiv \mathrm{Si} - \mathrm{H} \ + \ \mathrm{H}^{\circ} \tag{3}$$

Unfortunately, there exists one disadvantage. At room-temperature, the process is reversible because hydrogen will not create a stable bond with the E'-center. Therefore, the defects will be generated in a higher amount during the hydrogen-reduction due to outgassing.

Therefore, the UV-damage in the UVM-fibers with small core diameter (see below) will appear within days. However, these fibers can be used in small lengths, e.g. in fiber-bundles. As shown in Fig.1, the transmission will be reduced at 214 nm (maximum of E'-center) to approx. 45 % of the starting value. In many applications, this damage can be taken into account causing no problems.

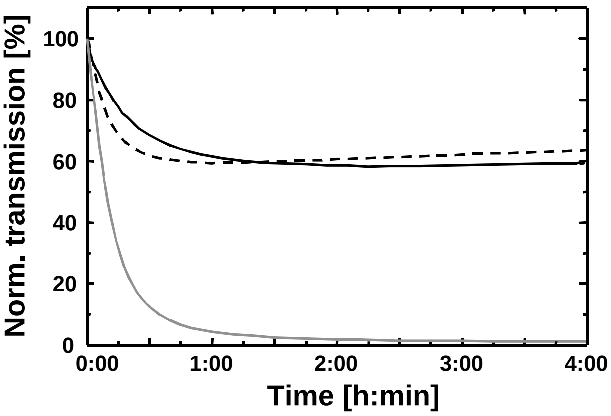

Fig. 1: Comparison of short-length (0.5m) hydrogen-free silica fibers having high-OH core: new UVM-quality with 70 and 100 µm core (upper curves) and standard-quality with 100 µm core (lower curve)

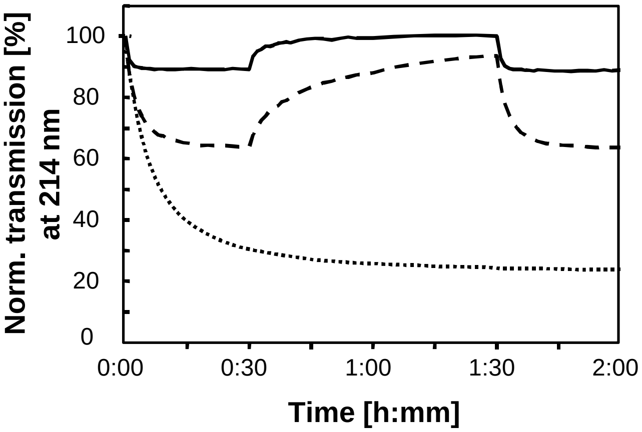

Fig.2: Short- and long-term degradation of hydrogen-loaded UVMI-fibers with 2.0 m length; hydrogen-level: very high at the beginning (upper curve), medium (middle curve) and small (lower curve)

In addition, the input power itself is important. In the unloaded UVM-fibers, the slope of degradation is influenced by the input power. Reducing the input power from 90 % down to 4.5 %, the grade of the slope at the beginning (t = 0 min) is reduced in the same magnitude of order. So, the defect concentration is proportional to the total energy. However, the saturation level differences are much smaller based on our measured data. This can be explained by the annealing process which runs parallel to the damaging process. On the other hand, the change in the lamp spectrum during this test sequence may have an influence to the saturation level, too.

The performance of **UVI-fibers** (no longer commercially available), drawn from standard preforms and loaded with hydrogen, has been described earlier /6/. Although the permanent defects were no longer observed, the modulation of transient defects was disturbing. In order to study this effect in more detail, we have used the cyclic test. After 0.5 hours of damage due to UV-irradiation of a deuterium-lamp, the fiber will recover over one hour because the UV-light will be switched off. In order to reduce the systematic errors due to dark signal drifts, we add another phase of UV-irradiation.
Directly after hydrogen-loading, the first phase of UV-light shows a decrease and increase of the UV-transmission in **UVM-fibers**; some of the precursors will be changed by the UV-light and passivated by hydrogen, afterwards. After this first “UV-treatment” (T = 0 d), the measured value for nearly all fiber diameters is in the range of less than 6 % (see Fig. 2). The starting value will be reached again, after a 1 hour recovery. Because the hydrogen moves out, the damaging curve looks similar to that curve of an UVM-fiber (Fig. 1). In this case, we used the test procedure for the UVM-fibers: 4 hours of continuous UV-irradiation.

Fig. 3 shows the normalized transmission at 214 nm wavelengths for UVMI-fibers with different core diameters, after saturation with UV-light. In addition, the gain in transmission is shown, too (t = 1.5 hours). All fibers show nearly the same behavior for different diameters and temperatures (Fig. 4), on a normalized time-axis.
It is obvious that with increasing diameter the lifetime of the fiber increases, too. Because the usage of the fiber and the requirement of the applications may be quite different, the determination of the fiber lifetime is difficult. Depending on the definition with deuterium-lamps (50% reduction), the lifetime of a 2 m long fiber can be predicted in dependence of the core diameter and the ambient temperature. At room-temperature (T= 22 ^{0}C), the following values have been either measured of calculated (see table 1); the calculations are based on the following equation:

$$t_{\,3dB}\,(CD,\,T) \;=\; 2.3\text{ months} * (D(22°C)/D(T)) * (CD/200\ \mu m)^2 \qquad (4),$$

with CD: core diameter
D(T): diffusion-coefficient for hydrogen in silica /17/.

However, reducing the fiber-length to 1 m, the lifetime will increase with approx. 50 %.

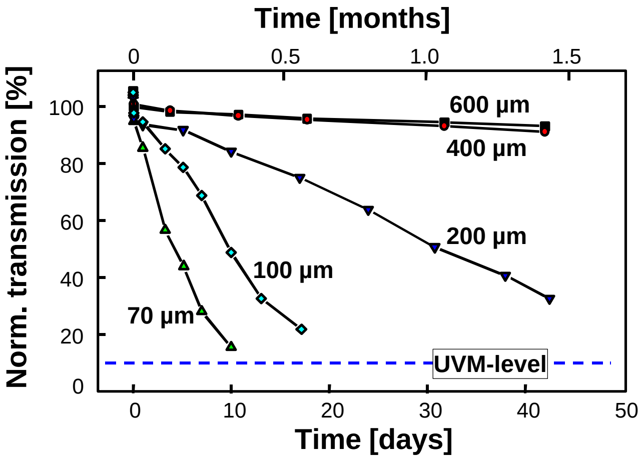

Fig. 3: Temporal degradation of 2 m long UVMI-fibers (after saturation with UV-light) with different diameters, at ambient temperature of 35 ^{0}C

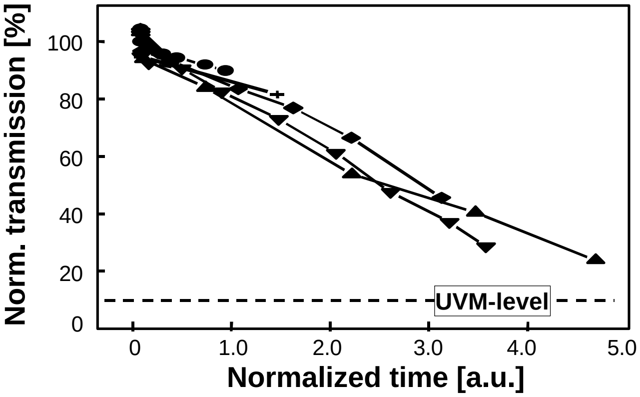

Fig. 4: same as Fig.3, but normalized in respect to temperature-dependent diffusion-coefficient and fiber-diameter

Table 1: Measured and predicted lifetime at room-temperature, based on eq. (2)

Core diameter [µm]:	70	100	200	400	600
lifetime [months]:	0.35	0.80	2.35	9.5	21.4

Other fiber-types with improved UV-performance are of great interest, too.

The improvement of the **UVI²-fiber** having 100 µm core diameter is an ongoing target. The best R&D-samples with optimized production-parameter showed a normalized transmission of 55 %, after saturation within 2 hours of UV-irradiation. In addition, no degradation of the saturation level has been observed over a period of 6 months. This fiber is an alternative for longer-length bundles.

The **few-mode fibers** with core diameters less than 35 µm were realized. The induced loss of a 1 m long non-loaded fiber at 214 nm wavelength was approx. 10 dB, using the deuterium-lamp for damaging. The defect-concentration is two times higher than the UVM-fiber. In the UV-region, this fiber can be used for laser-induced fluorescence in combination with the capillary electrophoresis application. So, the usefulness of the fiber has to be shown in the near future.

High-NA fibers in the DUV-region are commercially available. Using a high-OH silica core and a polymer cladding based on Teflon-AF /18/, a numerical aperture of 0.65 was realized. Unfortunately, the silica core is standard Suprasil /19/; so, the temporal UV-damage shows the same behavior like a UVI-fiber (all-silica) with the same core material /7/. Fig. 5 shows the measurement-results. After reaching the saturation level, no further degradation has been observed within the 15 hours of UV-irradiation. As a consequence, we can assert that the Teflon-material will not be damaged. But, only the low-order modes will be excited by the lamp-lens-system and selected by the spectrometer (NA: approx. 0.24). Therefore, this statement have to be confirmed in the near future by using the well-known differential mode methods in combination with excimer-lasers, as described for step-index fiber in /20/.

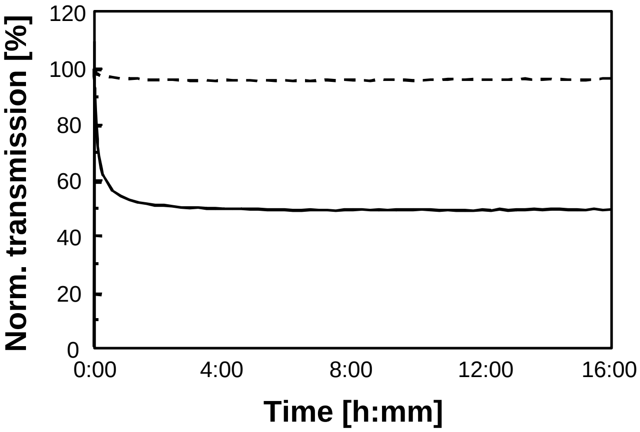

Fig. 5: UV-damage of a Teflon-coated UV-fiber with high-OH core material (Suprasil-quality /19/) at 214 nm (lower) and 266 nm (upper curve) loaded with hydrogen; core diameter: 400 µm, length: 2 m

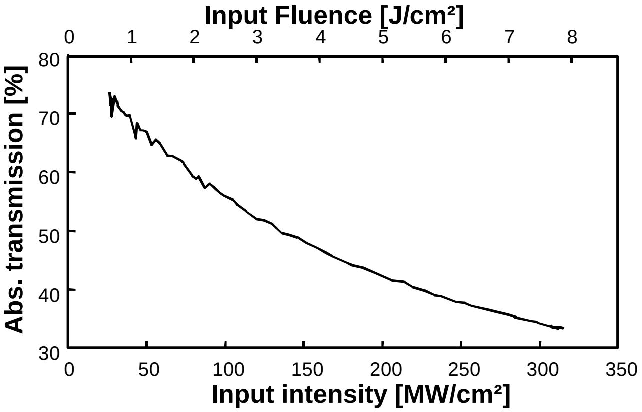

Fig. 6: Transmission at 248 nm wavelength (KrF-laser) in dependence of pulse energy or intensity at fiberfrontface, using UVMI-fiber

2.3 Experimental results with UV-lasers

In /11/, the non-loaded and loaded fibers drawn from a modified preform were tested with excimer-lasers, too. However, the power-level at the input was relatively small. Therefore, the nonlinear transmission was neglectable. In our studies, we wanted to show the improvement at power levels near the damage threshold /21/ in respect to the data presented in /22/.

In our tests, we used only 200 µm core fibers. At higher power-levels at the fiber input, the absolute transmission is no longer constant with a KrF-excimer laser at 248 nm, because the output pulse-energy and the output fluence are not linear with the comparable input parameters (Fig. 7).

Based on the equation (5), the linear and the non-linear absorption coefficients, α and β respectively, were determined (Fig. 8 and 9):

$$1/T = \{1 + I_0 * (\beta/\alpha)\} \exp(+\alpha z) - I_0 * (\beta/\alpha) \quad (5),$$

with: T: transmission
I_0: initial intensity at fiber input
z: fiber length.

For the first time, to our knowledge, these parameters could be determined with one fiber sample only because no transient losses due to UV-defects were observed. So, from the measured curve in Fig. 7 a constant linear coefficient could be calculated. The Fresnel-reflection was included in the model: the value of 4.6 % at both fiber endfaces leads to the best fit (Fig. 7). On the other hand, the non-linear coefficient was calculated not to be constant along the fiber (Fig. 8). Further studies are necessary to clearify the effects involved; perhaps, mode-conversion due to bending or Raman-scattering has to be taken into consideration.

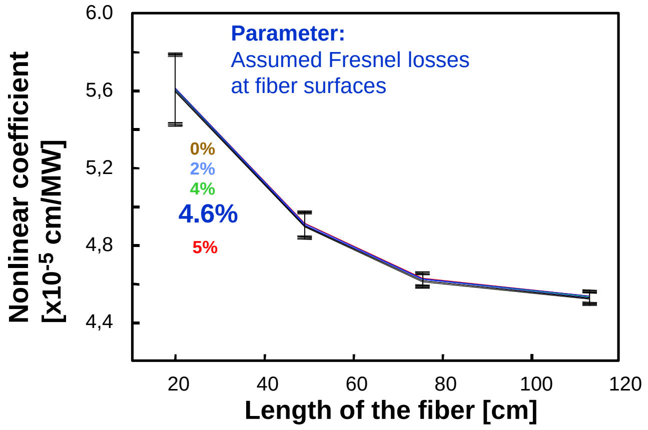

Fig. 7: Second order absorption-coefficient b in dependence of wavelength, determined at different fiber-lengths

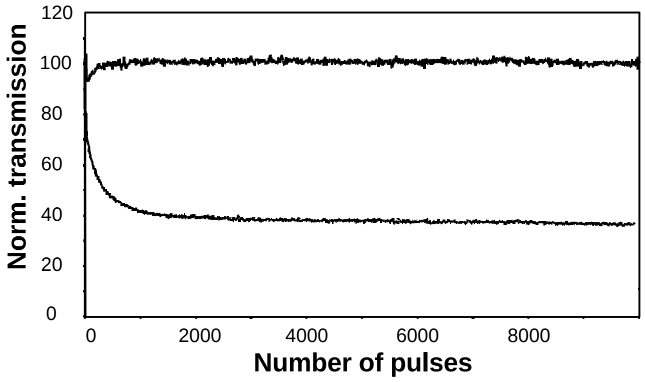

Fig.8: Improvement of temporal transmission at 193 nm (ArF-laser): UVMI-fiber (upper curve) and UVM-fiber (lower curve); core diameter: 200 µm, fiber-length: 0.30 m; laser fluence: 0.15 J/cm^2, pulse width: 25 ns

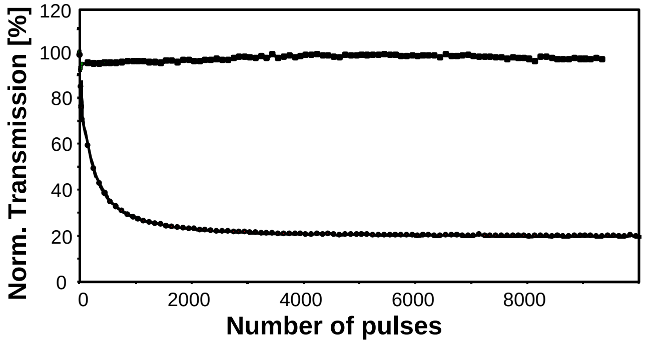

Fig.9: same as Fig.8, but at 213 nm wavelength (5th harmonic of Nd-YAG-laser) and fluence 0.10 cm^2, pulse width: 5 ns

Using a ArF-laser at 193 nm, the stronger suppression of the transient defects becomes obvious (Fig. 10). In comparison to the results presented in /22,23/, the transmission changes are less than 5 % in a 30 cm long sample, at 0.15 J/cm^2. The smaller fiber-length was chosen to avoid significant transmission losses due to two-photon-absorption. Two additional points are interesting. First, the loaded UVMI-fiber has a transmission minimum followed by an increase of transmission to nearly the starting level. Similar processes described above during UV-irradiation with deuterium-lamps play a role. Second, the non-loaded UVM-fiber has a surprisingly high transmission after saturation of 40 % in a 30 cm long sample.

For the first time, these fibers has been tested with a Nd-YAG-laser operating at 213 nm wavelength (5th harmonics). Again, the transient defects are significantly reduced compared to the results in /24/ using a frequency-doubled and tunable dyelaser. Only a small reduction of less than 5 % can be observed. Studies with longer length fiber will follow.

3. NEW APPLICATIONS WITH IMPROVED UV-SYSTEMS

With the new UVM- and UVMI-fibers, improvements of existing UV-systems or new applications are feasible.

The UV Resonant Raman Spectroscopy /25/ had been modified for measuring in liquids by using fiber-probes. Laser-light can be guided through the excitation fiber into the volume of interest in the liquid, while the Raman light is collected in the detection fibers which is connected to a spectrometer with high resolution. Because thicker-core fibers can be used, the UVMI-fibers are the right choice for this technique.

Parallel to that, laser-induced fluorescence spectroscopy can be miniaturized by using fibers /26/. Especially in combination with capillary electrophoresis, the UV-region is very important. In this case, the core diameter of the excitation fiber should be less than 50 µm; for low-power laser /13/, there will be no problems in respect to the stability during UV-transmission. In addition, the above described high-NA UV-fibers in combination with a photomultiplier (PMT) will collect significantly more light, so the signal-to-noise ratio (SNR) is higher.

Fig.10: Miniaturized dipping-probe in a 10mmx10mm cuvette

In combination with a liquid-core waveguide, on-line water measurements can be done /27/. In this case, two UVMI-fibers with 600 µm core can be used to transport the light from the deuterium-lamp to the analyte and from the analyte to the spectrometer. Several analytes with absorption bands below 220 nm have been measured, e.g. Toluene, nitrate and aspirin /28/.
An alternative for on-line liquid-measurements is a system with a miniature deuterium-lamp in combination with a miniaturized dipping-probe /29/; a small probe diameter of less than 1.5 mm can be demonstrated in a 10mmx10mm cuvette (Fig. 10)

The HPTLC-method (high performance thinlayer chromatography) is a well-known and versatile separation technique which shows several advantages to other chromatographic methods, especially in environmental analysis. Dirty samples can be screened without time-consuming pre-treatments. Some disadvantages of the commercially available systems can be avoided by using UV-fiber optics in combination with diode-array spectrometer; a non-expensive screening method for a large number of samples is feasible.

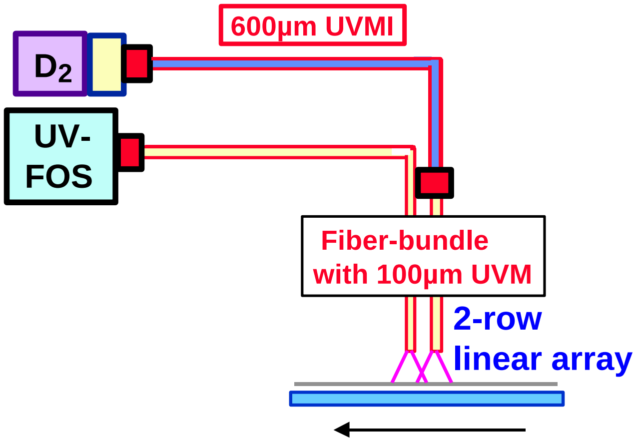

Fig.11: Equipment for diode-array TLC-method; description of components in the text

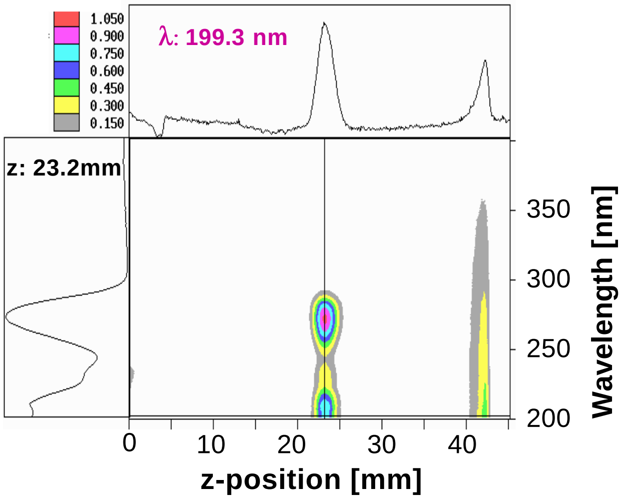

Fig.12: Example of DATLC: caffeine with absorption band at 199.3 nm: contour plot, chromatogram and spectrum of re-emission

The improved system (Fig. 11) contains a light source containing a standard deuterium-lamp and a halogen-lamp, a combination of a thick-core UVMI-fiber (core diameter: 600 µm) and two bundles of UVM-fibers (core diameter: 100 µm), and; a fiber-optic spectrometer /15/. In order to reduce the UV-induced losses below 250 nm, the UV-light of the deuterium-lamp will be guided through the UVMI-fiber, first. Then, the shorter first bundle of 22 UVM-fibers transfer the circular light-distribution of the first fiber into a linear shape on the plate. The second linear row of UVM-fibers in the assembly will collect the re-emitted light and transport it to the spectrometer. With this equipment, the spectral resolution was better than 1 nm in the wavelength region from 200 to 600 nm. The spatial resolution could be measured to be better than 150 µm depending on the chosen distance of the distal end of the assembly and the TLC-plate.
In addition to the polyaromatic hydrocarbons /29/ we have studied e.g. caffeine. The 100 ng probe was dabbed on a TLC-plate (Merck) using a mobile phase of Isopropanol (7parts), Cyclohexane (2 parts) and 25% NH_3

(1 part) for separation over a distance of 50 mm. The spatial and spectral results of the separation are shown in Fig. 12. In addition to the contour-plot, the 199.3nm-chromatogram at the top and the caffeine-spectrum at the side are shown. Obviously, the baseline and the shape of the curves can be measured with high precision.
At least, we want to point out that a combination of UVM- and UVMI-fibers may have superior properties in some applications.

4. ACKNOWLEDGEMENT

The author would like to thank his students (Michael Hübner, Ralf Arndt, Jan Assmus) and his cooperation partners (Georg Hillrichs, FH Merseburg: excimer-laser testing; Bernd Spangenberg, FH Offenburg: HPTLC-method; Gary Nelson and Jim Clarkin, Polymicro Technologies, Phoenix: fiber manufacturing).

5. REFERENCES

/1/ Y.Matsuura,T.Yamamoto,M.Miyagi: “Aluminium-hollow fiber delivery system for excimer lasers”. SPIE-Proc., Vol. 3911 (BiOS 2000), paper: 3911-40 (San Jose, Jan.2000)
/2/ Y.Matsuura,G.Takada,M.Miyagi: “Hollow fibers for Nd:YAG and excimer lasers”. SPIE-Proc. Vol. 3927 (LASE 2000), paper: 3927-16 (San Jose, Jan.2000)
/3/ K.-F.Klein,A.Mühlich: "Quarzglas für unterschiedliche Anwendungen im Bereich von 0.2 µm und 2.4 µm (in German)". VDI-Berichte 673, p.147-177. (Karlsruhe, March 1988)
/4/ H.Fabian,U.Grzesik,G.Hillrichs,W.Neu: „Reduction of photodegradation in optical fibers for excimer laser applications“. SPIE-Proc., Vol.1649 (BiOS’92), pp. 80 - 90 (Los Angeles, January 1992)
/5/ Polymicro Technologies LLC, Phoenix: Brochure about step-index fibers
/6/ K.F.Klein,P.Schliessmann,E.Smolka,M.Belz,W.J.O.Boyle,K.T.V.Grattan: "UV-stabilized silica based fiber for application around 200 nm wavelength". Sensors and Actuators B, Vol. 38-39, pp. 305-309 (1997)
/7/ K.-F.Klein, R.Kaminski,S.Hüttel, J.Kirchhof, S.Grimm, G.Nelson: "Lifetime improvements and of UV-improved fibers for new applicatons". SPIE-Proc.Vol. 3262C (BiOS’98), pp. 150-160 (San Jose, Jan. 1998)
/8/ D.L.Griscom: „Defect structures of glasses“. J.Non-Cryst. Solids., Vol. 73 pp. 51-78 (1985)
/9/ R.A.Weeks: “The many varieties of E´-centers: a review“. J.Non-Cryst.Solids, Vol.179, pp. 1-9 (1994)
/10/ K.-F.Klein,G.Hillrichs,P.Karlitschek,K.Mann: "Possibilities and limits of optical fibers for the transmission of excimer laser radiation". SPIE-Proc. Vol. 2966, pp. 564-573 (Boulder, Oct. 1996)
/11/ J.Vydra,G.Schötz: „Improved all-silica fibers for deep UV-applications“. SPIE-Proc. Vol. 3596 (BiOS’99), paper 3596-25 (San Jose, Jan. 99)
/12/ Heraeus Noblelight: Brochure about standard deuterium lamps and Fiberlight™
/13/ Crystal, Berlin: Brochure about low-power Nd:YAG-lasers for UV-applications
/14/ Zeiss, Jena: Brochure about fiber-optic spectrometers for UV-Vis-NIR-applications
/15/ J&M, Aalen: Brochure about fiber-optic spectrometers for UV-Vis-NIR-applications
/16/ J.Gombert, M.Ziegler, J. Assmus, K.F. Klein, G.Nelson,J.Clarkin, H.Pross, J.Kiefer: „Radiation-damage of all-silica fibers in the UV-region“. SPIE-Proc., Vol. 3596 (BiOS’99), pp.124-132 (San Jose, Jan. 1999)
/17/ R.W.Lee: Diffusion coefficient of hydrogen in silica“. J.Chem.Phys. Vol. 36, pp. 1062 (1962)
/18/ DuPont (USA): Product information about Teflon AF® 2400 (May 1989)
/19/ Heraeus Quarzglas: Brochures about Suprasil™ and Fluosil™ (tradenames)
/20/ A.Bernhardt,K.F.Klein,H.Fabian,U.Grzesik,H.Henschel,O.Köhn,H.U.Schmidt: „Excitation dependent radiation-induced losses in step-index fibers with undoped core“. SPIE-Proc.Vol.1791, paper 1791-32 (Boston 1992)
/21/ R.S.Taylor, K.E.Leopold, R.K.Brimacombe,S.Mihailov: "Dependence of the damage and transmission properties of fused silica fibers on the excimer laser wavelength". Appl.Optics, Vol. 27(15), p.3124-3134 (‘88)
/22/ K.-F.Klein,G.Hillrichs,P.Karlitschek,K.Mann: "Possibilities and limits of optical fibers for the transmission of excimer laser radiation". SPIE-Proc. Vol.2966 „Annual Boulder Damage Symposium“, S.564-573 (Boulder, Oct. 1996)
/23/ P.Karlitschek, G.Hillrichs,K.-F.Klein,U.Grzesik: “Improved UV-fiber for 193 nm excimer laser applications”. SPIE-Proc. Vol. 2677 (BiOS 96), pp. 127 - 134 (San Jose, Feb.1996)
/24/ K.F.Klein,L.S.Greek,H.G.Schulze,M.W.Blades,C.A.Haynes,R.F.B.Turner: „Fiber-guided tunable UV-laserlight system around 215 nm“. SPIE-Proc., Vol. 2977 (BiOS’97), paper 2977-14 (SanJose, February 1997)
/25/ H.G.Schulze, C.J.Barbosa, L.S.Greek, R.F.B.Turner, .A.Haynes, K.-F.Klein, M.W.Blades: „Advances in fiber-optic based UV resonance Raman spectroscopy techniques for anatomical and physiological investigations“. SPIE-Proc., Vol. 3608 (BiOS’99), pp.157-167 (San Jose, Jan. 1999)
/26/ G.Marowsky,F.Lewitzka,P.Karlitschek,U.Bünting,M.Niederkrueger: “Miniaturized laser-induced fluorescence system with fiber optic probe for the analysis of acromatic compounds”. SPIE-Proc.,Vol. 3539, pp- 2-9 (Boston, Nov. 1998)
/27/ K.-F.Klein,H.Rode,M.Belz,W.J.O.Boyle,K.T.V.Grattan: "Water quality measurement using fiber optics at wavelengths below 230 nm". SPIE-Proc. Vol. 2836, S. 186-194 (Denver Aug.1996)
/28/ K.-F.Klein, M.Belz, Dress, Franke, Boyle, KTV Grattan:"Ultra-sensitive detection system for fiber optic based UV spectroscopy". SPIE-Proc. Vol. 3258 (BiOS 98), paper 3258-11 (San Jose, Jan. 1998)
/29/ B.Spangenberg, K.-F.Klein: „Diode-Array HPTLC of PAHs“. Proc. InCom 99 - Instrumentalized Analytical Chemistry and Computer Technology - (Düsseldorf, März 1999)